

# On the heavy Majorana neutrino and light sneutrino contribution to $e^-e^- \rightarrow \ell^-\ell^-$ , ( $\ell = \mu, \tau$ )

M. Cannoni<sup>1,2,a</sup>, St. Kolb<sup>2</sup>, O. Panella<sup>2</sup>

<sup>1</sup> Dipartimento di Fisica, Università degli Studi di Perugia, Via A. Pascoli, 06123, Perugia, Italy

<sup>2</sup> Istituto Nazionale di Fisica Nucleare, Sezione di Perugia, Via A. Pascoli, 06123 Perugia, Italy

Received: 11 September 2002 / Revised version: 26 February 2003 /

Published online: 5 May 2003 – © Springer-Verlag / Società Italiana di Fisica 2003

**Abstract.** The cross section for the reaction  $e^-e^- \rightarrow \ell^-\ell^-$  ( $\ell = \mu, \tau$ ) is calculated in models with heavy Majorana neutrinos mediating lepton number violating amplitudes at the loop level. The contributing four-point functions are evaluated exactly (numerically) taking into account the full propagator dependence on external momenta, thereby extending to the energy range of interest for the next linear colliders an earlier approximate low energy calculation. The amplitude shows a non-decoupling behavior relative to the heavy Majorana neutrino masses, but due to the stringent bounds on heavy–light mixing the signal cross section attains observable values only for the less constrained  $\tau$  signal. The cross section induced by lepton number violation in the  $SU(2)_L$  doublet sneutrino sector of supersymmetric extensions of the standard model is constrained by the upper limits on neutrino masses and probably too tiny to be observable.

The process  $e^-e^- \rightarrow \ell^-\ell^-$  ( $\ell = \mu, \tau$ ), which violates the  $L_e$  and  $L_\ell$  lepton numbers, is forbidden in the standard model (SM) due to exact lepton number conservation to all orders of perturbation theory. Its observation at a next generation linear collider with center of mass energy  $\sqrt{s} = 500, 800, 1000$  GeV may be possible only if there is new physics that can trigger it. The signature is clear and practically free from SM background. In the literature it was studied:

- (i) in the context of models with gauge bileptons [1], where the final state is reached through tree level  $s$ -channel annihilation into a gauge bilepton and subsequent decay;
- (ii) in the context of mixing models where the reaction proceeds through a loop (box diagram) with heavy Majorana neutrinos and  $W^-$  gauge bosons as virtual particles running in the loop [2], and
- (iii) in supersymmetric scenarios where sneutrinos and charginos instead of neutrinos and charged bosons are exchanged [3].

The aim of this paper is

- (i) to improve and extend the calculation of [2] (which was essentially a low energy calculation) in order to provide predictions in the energy range of interest for the next linear collider project, motivated by the observation that all diagrams of the process, see Fig. 1a–d, have a threshold singularity at  $\sqrt{s} = 2M_W$  where the amplitude develops an imaginary part giving a boost to its absolute value (see the well known example of photon–photon scattering [4]),

taking also into account experimental bounds on effective mixing angles not considered in [2];

- (ii) to make a realistic calculation for the sneutrino case: the cross section was estimated so far assuming eV scale sneutrinos [3].

We assume that heavy Majorana neutrinos (mass eigenstates) couple to the standard model charged currents through heavy–light neutrino mixing. This is the simplest way to obtain lepton number violating processes. Consider the box diagrams depicted in Fig. 1a–d. As in [2], we use the 't Hooft–Feynman gauge: there are graphs with  $WW$ ,  $\phi\phi$  and  $\phi W$  exchange,  $\phi$  being the Goldstone boson. The lagrangian of interest is [15]

$$\mathcal{L} = \sum_{\ell, N_i} -i \frac{g}{\sqrt{2}} \left[ \bar{\psi}_\ell \gamma_\mu \frac{1 - \gamma_5}{2} U_{\ell N_i} \psi_{N_i} W^\mu - \frac{M_{N_i}}{M_W} \bar{\psi}_\ell \frac{1 + \gamma_5}{2} U_{\ell N_i} \psi_{N_i} \phi \right] + \text{h.c.} \quad (1)$$

where  $\ell = e, \mu, \tau$  and  $U_{\ell N_i}$  are the elements of the mixing matrix of the heavy mass eigenstates  $M_{N_i}$  labeled by the index  $N_i$ . Neglecting the masses of the external particles allows one to simplify the calculation of the amplitudes that can be expressed in terms of

- (i) the Mandelstam variables  $s$ ,  $t$  and  $u$ ;
- (ii) the spinor products of light-like momenta (see [5] and references therein)

$$\begin{aligned} S(p_a, p_b) &= \bar{u}_+(p_a) \cdot u_-(p_b), \\ T(p_a, p_b) &= \bar{u}_-(p_a) \cdot u_+(p_b), \end{aligned} \quad (2)$$

<sup>a</sup> e-mail: mirco.cannoni@pg.infn.it

which obey the relation:  $|S(p_2, p_1)T(p_3, p_4)|^2 = s^2$ ; and (iii) the scalar  $D_0$  and the tensor rank-1 ( $D_\mu$ ) and rank-2 ( $D_{\mu\nu}$ ) four-point functions [6].

The corresponding amplitudes are found to be

$$\mathcal{M}_a^{WW} = \left(\frac{g}{\sqrt{2}}\right)^4 \frac{1}{(4\pi)^2} \sum_{N_i, N_j} (U_{eN_i}^* U_{\mu N_j})^2 M_{N_i} M_{N_j} \times 4S(p_2, p_1)T(p_3, p_4) [D_0(s, t) + D_0(s, u)], \quad (3)$$

$$\mathcal{M}_b^{\phi\phi} = \left(\frac{g}{\sqrt{2}}\right)^4 \frac{1}{(4\pi)^2} \sum_{N_i, N_j} (U_{eN_i}^* U_{\mu N_j})^2 \frac{M_{N_i}^2 M_{N_j}^2}{M_W^2 M_W^2} \times M_{N_i} M_{N_j} S(p_2, p_1)T(p_3, p_4) [D_0(s, t) + D_0(s, u)], \quad (4)$$

$$\mathcal{M}_c^{W\phi} = \left(\frac{g}{\sqrt{2}}\right)^4 \frac{1}{(4\pi)^2} \sum_{N_i, N_j} (U_{eN_i}^* U_{\mu N_j})^2 \frac{M_{N_i} M_{N_j}}{M_W M_W} \times S(p_2, p_1)T(p_3, p_4) \left[ 4(D_{00}(s, t) + D_{00}(s, u)) - 2(tG(s, t) + uG(s, u)) - 2(tV(s, t) + uV(s, u)) \right], \quad (5)$$

$$\mathcal{M}_d^{\phi W} = \left(\frac{g}{\sqrt{2}}\right)^4 \frac{1}{(4\pi)^2} \sum_{N_i, N_j} (U_{eN_i}^* U_{\mu N_j})^2 \frac{M_{N_i} M_{N_j}}{M_W M_W} \times S(p_2, p_1)T(p_3, p_4) \left[ 4(D_{00}(s, t) + D_{00}(s, u)) - 2(tG(s, t) + uG(s, u)) \right]. \quad (6)$$

The numerical computation of the four-point functions was performed using the LOOPTOOLS software [7], where the following notation is used as regards the expansion of the rank-1 and rank-2 tensor functions:  $D_\mu = \sum_{i=1}^3 D_i(k_i)_\mu$ ,  $D_{\mu\nu} = g_{\mu\nu}D_{00} + \sum_{i,j=1}^3 D_{ij}(k_i)_\mu(k_j)_\nu$ ,  $k_i$  being sums of external momenta running in the loop as explained in Fig. 1f. Within this notation the form factors  $G$  and  $V$  appearing in (3)–(6) are given by

$$G = D_{22} + D_{23} + D_{12} + D_{13}, \\ V = 2D_2 + D_1 + D_3 + D_0.$$

Terms depending both on  $(s, t)$  and  $(s, u)$  appear because the identical fermions in the final state require proper antisymmetrization of the amplitudes. Defining  $x_W = \sin^2 \theta_W$  and  $x_{i,j} = M_{N_{i,j}}^2 / M_W^2$ , the differential cross section is easily found to be

$$\frac{d\sigma}{d\cos\theta} = \frac{1}{256\pi} \left(\frac{\alpha}{x_W}\right)^4 |K(s, t, u)|^2 s, \quad (7)$$

where  $K$  is given by

$$K = \sum_{N_i, N_j} (U_{eN_i}^* U_{\mu N_j})^2 \sqrt{x_i x_j} \left\{ M_W^2 \left(1 + \frac{x_i x_j}{4}\right) \times [D_0(s, t) + D_0(s, u)] + 2(D_{00}(s, t) + D_{00}(s, u)) - [tG(s, t) + uG(s, u)] - \frac{[tV(s, t) + uV(s, u)]}{2} \right\}. \quad (8)$$

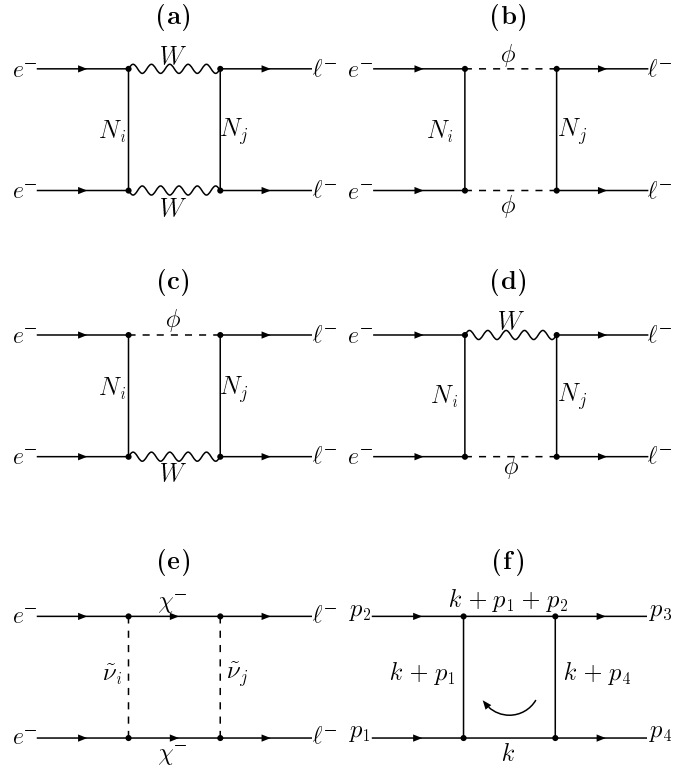


**Fig. 1a–f.** In **a–d** we show the Feynman diagrams, in the 't Hooft–Feynman gauge, contributing to  $e^-e^- \rightarrow \ell^-\ell^-$  ( $\ell = \mu, \tau$ ) via heavy Majorana neutrinos. In **e** the corresponding SUSY diagram is given which arises in models with lepton number violation in the sneutrino sector. In **f** the choice of the running momentum is given. The momenta  $k_i$  ( $i = 1, 2, 3$ ) for the decomposition of the tensor integrals within the LOOPTOOLS notation are  $k_1 = p_1$ ,  $k_2 = p_1 + p_2$ ,  $k_3 = p_1 + p_2 - p_3 = p_4$

To obtain the total signal cross section  $\sigma_{\text{tot}}$ , (7) is integrated numerically over the scattering angle in the center of mass frame. As stated above, similar formulas were obtained in [2] using the approximation where *all external momenta in the loops are neglected* relative to the heavy masses of the gauge bosons and Majorana neutrinos, enabling one to carry out the loop integration analytically. The formulas thus obtained are well known in the literature [8] and the final cross section, which depends only on  $x_{i,j}$  and the mixing coefficients, grows linearly with the center of mass energy squared,  $s$ . This approximation for the four-point functions is good at low energies, such as in decay processes of heavy mesons, or when  $\sqrt{s} \ll M$ ,  $M$  being the highest mass running in the loop. In addition the linear growth with  $s$  would break unitarity, therefore in order to make quantitative predictions with the correct high energy behavior, the four-point functions full dependence on the external momenta has to be considered. Theoretically, according to the ‘‘Cutkosky rule’’, one expects an enhancement at  $\sqrt{s} \simeq 161 \text{ GeV} \simeq 2M_W$ , the threshold for on-shell  $WW$  gauge boson production, at which the four-point functions develop an imaginary part. In Fig. 2a the ratio  $R_\sigma = \sigma_{\text{tot}}/\sigma_0$  of the integrated total cross section  $\sigma_{\text{tot}}$  to  $\sigma_0$ , the cross section of the low energy calculation

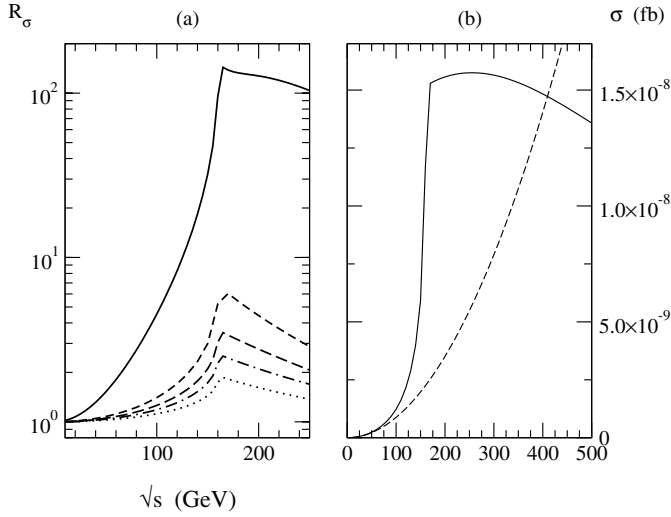


**Fig. 2a,b.** In **a** the ratio  $R_\sigma$  is plotted as a function of  $\sqrt{s}$  the energy in the center of mass system: solid line,  $M_{N_i} = M_{N_j} = 100$  GeV; short-dashed line,  $M_{N_i} = 150$  GeV,  $M_{N_j} = 450$  GeV; long-dashed line,  $M_{N_i} = M_{N_j} = 500$  GeV; dot-dashed line,  $M_{N_i} = M_{N_j} = 1$  TeV; dotted line,  $M_{N_i} = M_{N_j} = 3$  TeV. In **b** the absolute values of the cross sections are given for a particular choice of Majorana masses  $M_{N_i} = 150$  GeV,  $M_{N_j} = 450$  as function of the energy in the center of mass frame. The solid line is obtained integrating (7) while the dashed line is based on (9) of [2]

of [2], is plotted for sample values of the Majorana masses. The enhancement due to the threshold singularity of the loop amplitude is more pronounced for values of Majorana masses close to  $M_W$  and is drastically reduced increasing  $M_{N_i} \approx M_{N_j}$  to  $\mathcal{O}(\text{TeV})$ . As  $R_\sigma \rightarrow 1$  as  $\sqrt{s} \ll M_W$  in all the cases, the agreement of our full calculation with the result of [2] in the regime of low energies is evident<sup>1</sup>.

The threshold effect appears to be quite spectacular only for values of Majorana masses that correspond to cross sections too small to be measured even at a next linear collider. In Fig. 2b the effect of the threshold singularity in the loop integral is shown reporting absolute cross sections for a particular choice of Majorana masses:  $M_{N_i} = 150$  GeV and  $M_{N_j} = 450$  GeV. The low energy approximation (dashed line) obtained neglecting external momenta in the loop is inadequate when the energy of the reaction increases to values comparable with the masses. Increasing the energy, after reaching a maximum, the cross section starts to decrease until the asymptotic behavior  $\mathcal{O}(1/s^2)$  of the loop integral  $K$  is reached. This happens for every value of heavy Majorana neutrino masses and we checked numerically that, as expected, for higher masses the asymptotic regime is reached at higher values of  $\sqrt{s}$ . In fact from Fig. 3 we note that the cross section grows with

<sup>1</sup> It should be mentioned that the agreement, at low energies, of our (7) with (9) of [2] is up to a factor of 4. We have contacted the author of [2] on this matter and he agrees with our (7). That is, (9) of [2] should be divided by 4 (in [2] the average over initial spins was left out [9]) and then for energies  $\sqrt{s} \ll M_W$  it coincides exactly with our (7)

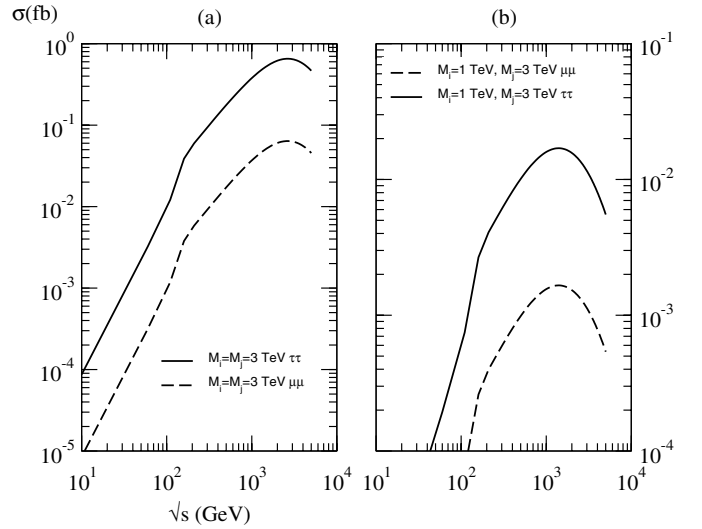


**Fig. 3a,b.** Total cross sections as function of the center of mass energy,  $\sqrt{s}$ . The value of the mixing coefficients are discussed in the text. In part **a** the solid curve refers to the case of  $e^-e^- \rightarrow \tau^-\tau^-$  with  $M_{N_i} = M_{N_j} = 3$  TeV, while the dashed line refers to  $(e^-e^- \rightarrow \mu\mu)$  with the same values of Majorana masses. In **b** the Majorana masses are changed to somewhat lower values:  $M_{N_i} = 1$  TeV,  $M_{N_j} = 3$  TeV

increasing HMN masses. The main contribution comes from the graph with two Goldstone bosons since their coupling is proportional to  $M_{N_i}$ . Moreover the chiral structure of the coupling selects the mass term in the numerator of the Majorana neutrino propagators. When these masses are much larger than the other quantities, the amplitude scales like  $M_{N_i}^3 M_{N_j}^3 / M_{N_i}^2 M_{N_j}^2 \simeq M_{N_i} M_{N_j}$ , i.e. is proportional to the square of the heavy masses. This fact is the well known non-decoupling of heavy fermions in theories with spontaneous symmetry breaking (similarly in the SM the top quark gives sizable radiative corrections owing to its large mass and a quadratic non-decoupling).

Heavy Majorana neutrinos naturally appear in extensions of the SM with right-handed neutrinos which generate light neutrino masses through the see-saw mechanism. The scale of the masses  $M_R$  is of order  $10^{9-12}$  GeV with very small heavy-light mixing,  $U_{\ell j} \sim M_{N_j}^{-1}$ , and the cross section will be suppressed by inverse powers of these masses, thus recovering the decoupling limit that is natural in the see-saw framework.

An interesting scenario is the model recently proposed in [24], where an attempt is made to construct light neutrino masses with a see-saw mechanism and no new physics beyond the TeV scale. This is achieved by adding a new Higgs doublet, relative to the SM, whose neutral component develops a naturally small vacuum expectation value,  $u \sim 1$  MeV, so that  $m_\nu = m_D^2 / M_N = f^2 u^2 / M_N \sim 1$  eV if  $M_N \sim 1$  TeV and  $f \sim 1$ , with  $f$  being the Yukawa coupling. But the heavy-light mixing is  $\sim fu / M_N \sim 10^{-6}$ , which is too small to have phenomenological consequences. Further it was shown in [25] that a charged Higgs boson of this model must be heavier than 50 TeV, in order to

satisfy the experimental bound of the  $\mu \rightarrow 3e$  decay. So this model does not comply with the constraints from non-observation of lepton flavor violation.

More interesting from the phenomenological point of view is the case in which HMN have masses in the TeV range with non-negligible mixing. Mass matrices that satisfy this condition can be built, using experimental constraints on heavy–light mixing (including those from  $\beta\beta_{0\nu}$  [11]). This is achieved imposing relations among the elements of the neutrino mass matrix in a way that the mixing is decoupled from mass relations and is bounded only by data [12,13]. Independence of the mixing matrix from the mass relation and the consequent possibility of violating the Appelquist–Carazzone theorem [14] have led many authors to study HMN contributions to rare processes like  $\mu \rightarrow e\gamma$ ,  $\mu \rightarrow e^+e^-e^-$  [10,13,15–19]. However it was recently argued in [11] that even if such a situation is not still ruled out by present data on neutrino oscillations, it requires extreme fine tuning among the elements of the Dirac mass matrix  $m_D$  and those of  $M_R$ . Keeping this in mind, we can nonetheless explore the phenomenological consequences of such a scenario. As was done in [5] we take the following experimental upper bounds on effective heavy–light mixing [20,21,11]:

$$\begin{aligned} s_{\nu_e}^2 &= \sum_{N_i} |U_{eN_i}|^2 < 0.0027, \\ s_{\nu_\mu}^2 &= \sum_{N_i} |U_{\mu N_i}|^2 < 0.005, \\ s_{\nu_\tau}^2 &= \sum_{N_i} |U_{\tau N_i}|^2 < 0.016, \end{aligned} \quad (9)$$

and allow the heavy Majorana masses to vary in the TeV range. Thus mixing coefficients as large as advocated in [2],  $(U_{eN_i}U_{\mu N_j})^2 \simeq 10^{-1}–10^{-2}$ , could only arise in unnatural and fine tuned models [22]. Note that, approximately, the cross section goes like  $(s_{\nu_e}^2)^2(s_{\nu_\mu}^2)^2$ , for real matrix elements. In this context, the coupling of HMN to gauge bosons and leptons is fixed to  $gU_{\ell N_i}$ , where  $g$  is the  $SU(2)$  gauge coupling of the SM. Since the width of HMN grows with  $M_N^3$ , at a certain value it will happen that  $\Gamma_N > M_N$ , signaling a breakdown of perturbation theory. The perturbative limit on  $M_N$  is thereby estimated requiring  $\Gamma_N < M_N/2$ , which gives an upper bound of  $\simeq 3$  TeV [15,23].

In Fig. 3a the cross section is plotted for masses up to this perturbative limit, using the maximally allowed value of the mixing. We see that for  $M_{N_i} = M_{N_j} = 3$  TeV the signal does reach the level of  $10^{-1}$ ,  $10^{-2}$  fb respectively for the  $(\tau\tau)$  and the  $(\mu\mu)$  signals at  $\sqrt{s} = 500$  GeV, which for an annual integrated luminosity of  $100 \text{ fb}^{-1}$  would correspond respectively to 10 and 1 event/year. At higher energies,  $\mathcal{O}(\text{TeV})$ , one could get even larger event rates (30 and 3) respectively. The solid curve refers to  $e^-e^- \rightarrow \tau^-\tau^-$ : this is largest because the upper limits on the mixing are less stringent. One can also see the onset of the asymptotic regime at  $\sqrt{s} \approx 3$  TeV. Figure 3b shows that the cross section quickly decreases as lower Majorana masses are considered.

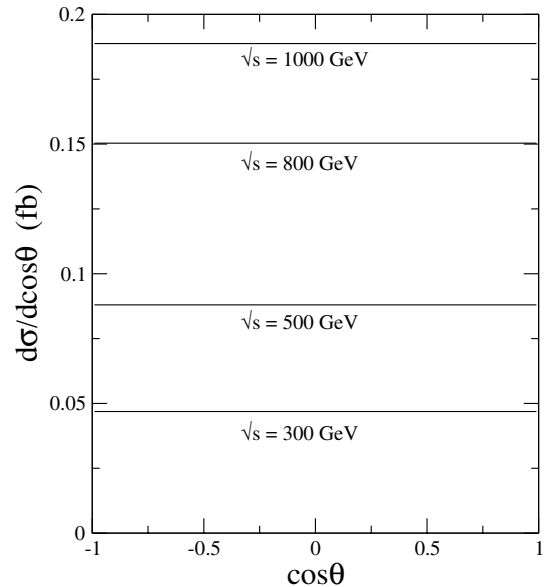


**Fig. 4.** Angular distribution in the polar angle of the outgoing lepton for different values of the center of mass energy,  $\sqrt{s}$  in the case of  $e^-e^- \rightarrow \tau^-\tau^-$  with  $M_{N_i} = M_{N_j} = 3$  TeV. The curves are not exactly constant, and using an appropriate scale they show small deviations from a straight line, remaining left–right symmetric

As even in the more optimistic cases event rates are quite modest it is important to check how the signal cross section is affected by kinematic cuts on the angle of the outgoing leptons. The angular distributions turn out to be practically constant as shown in Fig. 4. They are forward–backward symmetric because both the  $t$ - and  $u$ -channel are present. The absence of a strong dependence on the polar angle is due to the fact that within the range of the parameters used here the contributing four-point functions depend very mildly on the kinematic variables ( $u$  and  $t$ ).

This behavior can be most easily understood using helicity amplitudes. The spinorial part common to all the diagrams is

$$[\bar{v}(p_2)P_L u(p_1)] [\bar{u}(p_3)P_R v(p_4)] = S(p_2, p_1)T(p_3, p_4), \quad (10)$$

that in the limit of massless external particles is a well defined helicity amplitude:  $e_L e_L \rightarrow \ell_L \ell_L$ . In the center of mass frame this is a S-wave scattering with  $J_z = 0$ , meaning that the scattered particles are emitted back to back but without a preferred direction relative to the collision axis ( $z$ ).

So this signal is characterized by practically flat angular distributions and as a result the total cross section is quite insensitive to angular cuts. Values of  $\sigma_T$  for different angular cuts are reported in Table 1. With  $|\cos\theta| \leq 0.99$  the change in  $\sigma_T$  is  $\approx 1\%$  for all energies considered, while using  $|\cos\theta| \leq 0.95$  the total cross section decreases by  $\approx 5\%$ . Note that the reduction of the total cross section is measured almost precisely by the reduction of the phase space, meaning that the angular distribution is constant up to  $\approx 0.1\%$ . Thus it can be concluded that the number

**Table 1.** Total cross section (for two different angular cuts) at some sample energies. The corresponding cuts on the transverse momentum of outgoing leptons are also shown. The numerical values for masses and mixing correspond to the solid line of Figs. 3a and 4

	$\sqrt{s} = 300 \text{ GeV}$	$\sqrt{s} = 500 \text{ GeV}$	$\sqrt{s} = 800 \text{ GeV}$	$\sqrt{s} = 1000 \text{ GeV}$
	$\sigma \text{ (fb)}$	$\sigma \text{ (fb)}$	$\sigma \text{ (fb)}$	$\sigma \text{ (fb)}$
$ \cos \theta  \leq 1$	0.094	0.176	0.301	0.379
$ \cos \theta  \leq 0.99$	0.093	0.174	0.297	0.374
$ \cos \theta  \leq 0.95$	0.089	0.167	0.285	0.358

of events will not be drastically affected for any reasonable choice of experimental cuts.

In supersymmetric (SUSY) extensions of the see-saw framework (see e.g. [26]) the natural mass scale of the singlet neutrino sector is at least of order  $\mathcal{O}(10^{12})$  GeV: in a unified scenario such a value improves the unification of gauge coupling constants [27]. Therefore HMN masses in the TeV range – although not ruled out experimentally – are disfavored from a model building point of view. In the effective low energy SUSY see-saw framework, however,  $L$  is violated by the light  $SU(2)_L$  doublet sneutrinos [3, 28, 29, 26]. The mass states  $\tilde{\nu}_{\ell_{1,2}}$  ( $\ell$  denotes the generation) exhibit a mass-splitting  $\Delta m_\ell = m_{\ell_1} - m_{\ell_2}$  that is constrained by its radiative contribution to neutrino masses [30]:  $\Delta m_\ell < 36(156)(m_\ell^{\text{exp}}/1 \text{ eV}) \text{ keV}$  for a common scale of SUSY masses of 100 GeV, and  $m_\ell^{\text{exp}}$  the experimental limits on neutrino masses. The two different values refer to average and absolute upper limits when scanning over the SUSY parameter space. Then, in addition to the HMN mediated contribution discussed above, a diagram containing  $L$ -violating doublet sneutrinos and charginos is present; see Fig. 1e. The  $L$ -violating doublet sneutrino propagator and hence the resulting cross section is proportional to  $\Delta m$ . Such a contribution has been considered in [3] for the case of eV scale sneutrinos. In the realistic case of  $\mathcal{O}(100)$  GeV scale sneutrinos, the exact differential cross section, in the notation of Fig. 1f for the momenta, is

$$\frac{d\sigma}{d\cos\theta} = \frac{1}{128\pi} \left( \frac{\alpha}{x_W} \right)^4 \left| 2 \left[ D_{00}(s, t) + D_{00}(s, u) \right] - \left[ uA(s, t) + tA(s, u) \right] \right|^2 s, \quad (11)$$

$$A = D_2 + \sum_{i=1}^3 D_{2i}.$$

Here, the sum over the (maximally mixed) individual mass states in the  $L$ -violating sneutrino propagators is included in the loop coefficients  $D_{00}$  and  $A$ , and the chargino is assumed to be a pure gaugino. In Fig. 5 the resulting total  $\mu^- \mu^- \rightarrow \tau^- \tau^-$  cross section is plotted for a common SUSY mass  $(m_1 + m_2)/2 \equiv \bar{m}_\ell = m_\chi = 100 \text{ GeV}$  and for (maximal) values  $\Delta m_\mu = 30 \text{ GeV}$  and  $\Delta m_\tau = 80 \text{ GeV}$  ( $\Delta m_\ell$  must not exceed  $\bar{m}_\ell$ , otherwise the vacuum becomes unstable [29]) allowed by the *kinematic* upper limits on the neutrino masses [31]  $m_\mu < 190 \text{ keV}$  and  $m_\tau < 18.2 \text{ MeV}$ . Even for such unrealistically large neutrino masses and,

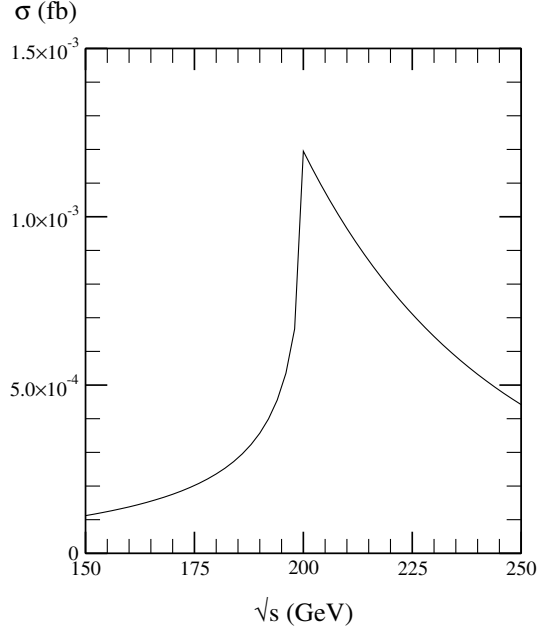


**Fig. 5.** Total cross section for the sneutrino mediated reaction  $\mu^- \mu^- \rightarrow \tau^- \tau^-$ . The plot refers to the following choice of parameters:  $\Delta m_\mu = 30 \text{ GeV}$  and  $\Delta m_\tau = 80 \text{ GeV}$ ,  $\bar{m} = m_\chi = 100 \text{ GeV}$

correspondingly, unrealistic values for the sneutrino mass-splitting, the maximal cross section, at the threshold singularity for real  $\chi^- \chi^-$  production, is of order  $\mathcal{O}(10^{-3})$  fb and therefore too small to be observable even for a nominal integrated luminosity of  $100 \text{ fb}^{-1}/\text{yr}$ . The cross section with two colliding electrons is even smaller because  $m_e^{\text{exp}} < 3 \text{ eV}$ . Unlike the Majorana neutrino mediated contribution the SUSY cross section decreases for larger values of  $\bar{m}_\ell$ . Since the reaction  $e^- e^- \rightarrow \ell^- \ell^-$  conserves total lepton number, processes like  $e^- e^- \rightarrow e^- \mu^-$  may arise due to interactions violating lepton flavor number but conserving the overall lepton number. This type of process will be discussed in the SUSY framework in a forthcoming paper [32].

Concluding, we have calculated the cross section for the process  $e^- e^- \rightarrow \ell^- \ell^-$  ( $\ell = \mu, \tau$ ) keeping the full dependence on the external momenta in the loop calculation and using the maximal value of effective light–heavy mixing angles allowed by experiments. We find that only for Majorana masses in the TeV range the reaction has

a measurable cross section (above  $10^{-2}$  fb) with better prospect for the  $\tau$  signal (the corresponding mixing coefficients being the less constrained), thereby arriving at somewhat less optimistic conclusions than in [2]. We have also estimated the corresponding SUSY contribution arising from sneutrino mixing. This, although it is affected by an enhancement in the region of the threshold singularity, remains below the minimal observable value of  $10^{-2}$  fb even for the (unrealistic) maximal value of sneutrino mass-splitting.

*Acknowledgements.* The work of St. Kolb is supported by the European Union, under contract No. HPMF-CT-2000-00752. The authors wish to thank X.Y. Pham for checking out his calculation of [2].

## References

1. P.H. Frampton, A. Rasin, Phys. Lett. B **482**, 129 (2000); M. Raidal, Phys. Rev. D **57**, 2013 (1998)
2. X.Y. Pham, Phys. Lett. B **495**, 131 (2000)
3. A. Halprin, Phys. Lett. B **151**, 372 (1984)
4. L.D. Landau, E.M. Lifshitz, Quantum electrodynamics (Pergamon Press, Oxford 1982), p. 572
5. O. Panella, M. Cannoni, C. Carimalo, Y.N. Srivastava, Phys. Rev. D **65**, 035005 (2002)
6. G. 't Hooft, M.J.G. Veltman, Nucl. Phys. B **153**, 365 (1979); G. Passarino, M. Veltman, Nucl. Phys. B **160**, 15 (1979)
7. T. Hahn, M. Perez-Victoria, Comput. Phys. Commun. **118**, 153 (1999)
8. T. Inami, C.S. Lim, Prog. Theor. Phys. **65**, 297 (1981); Erratum **65**, 1772 (1981)
9. X.Y. Pham, private communication
10. T.P. Cheng, L.F. Li, Phys. Rev. D **44**, 1502 (1991)
11. J. Gluza, hep-ph/0201002
12. W. Buchmuller, C. Greub, Nucl. Phys. B **363**, 345 (1991)
13. L.N. Chang, D. Ng, J.N. Ng, Phys. Rev. D **50**, 4589 (1994)
14. T. Appelquist, J. Carazzone, Phys. Rev. D **11**, 2856 (1975)
15. A. Ilakovac, A. Pilaftsis, Nucl. Phys. B **437**, 491 (1995)
16. A. Ilakovac, B.A. Kniehl, A. Pilaftsis, Phys. Rev. D **52**, 3993 (1995)
17. D. Tommasini, G. Barenboim, J. Bernabeu, C. Jarlskog, Nucl. Phys. B **444**, 451 (1995)
18. P. Kalyniak, I. Melo, Phys. Rev. D **55**, 1453 (1997)
19. G. Cvetič, C. Dib, C.S. Kim, J.D. Kim, Phys. Rev. D **66**, 034008 (2002)
20. E. Nardi, E. Roulet, D. Tommasini, Phys. Lett. B **327**, 319 (1994); **344**, 225 (1995)
21. S. Bergmann, A. Kagan, Nucl. Phys. B **538**, 368 (1999)
22. G. Belanger, F. Boudjema, D. London, H. Nadeau, Phys. Rev. D **53**, 6292 (1996)
23. J.I. Illana, T. Riemann, Phys. Rev. D **63**, 053004 (2001)
24. E. Ma, Phys. Rev. Lett. **86**, 2502 (2001)
25. M. Jamil Aslam, hep-ph/0203045
26. Y. Grossman, H.E. Haber, Phys. Rev. Lett. **78**, 3438 (1997)
27. J.A. Casas, J.R. Espinosa, A. Ibarra, I. Navarro, Phys. Rev. D **63**, 097302 (2001)
28. G.K. Leontaris, K. Tamvakis, J.D. Vergados, Phys. Lett. B **171**, 412 (1986)
29. M. Hirsch, H.V. Klapdor-Kleingrothaus, S. Kovalenko, Phys. Lett. B **398**, 311 (1997)
30. M. Hirsch, H.V. Klapdor-Kleingrothaus, S. Kovalenko, Phys. Rev. D **57**, 1947 (1998)
31. K. Hagiwara et al., Review of particle physics, Phys. Rev. D **66**, 010001 (2002)
32. M. Cannoni, St. Kolb, O. Panella, in preparation